© 2018 IJSRST | Volume 4 | Issue 5 | Print ISSN: 2395-6011 | Online ISSN: 2395-602X
Themed Section: Science and Technology

# Synthesis, Growth, Physicochemical Properties and DFT Calculations on Nonlinear Optical Single Crystal of L-Histidine Dinitrate for Frequency Conversion Applications

**K. Deepa[1], S. Senthil[2] , J. Madhavan*[1]**
[1]Department of Physics, Loyola College, Chennai, Tamil Nadu, India
[2]Department of Physics, Government Arts College for Men, Nandanam, Chennai, Tamil Nadu, India

## ABSTRACT

Single crystals of L-Histidine Dinitrate (LHDN) have been successfully grown by slow solvent evaporation technique at room temperature. Powder X-Ray diffraction patterns has been recorded and indexed for the analysis of crystalline nature and the lattice parameters of the grown crystals. L-Histidine Dinitrate crystallizes in orthorhombic space group $P2_12_12_1$ and it exhibit second order non-linear optical (NLO) susceptibility due to the intermolecular charge transfer. The functional groups are identified by Fourier transform infrared spectral analysis and compared with theoretical spectrum. The optical transmission range of the LHDN crystal has measured by UV–Vis–NIR studies. It is observed that the minimum absorption in the entire visible and ultra violet range of 240–1500 nm. From absorption spectra the optical band gap is found to be 4.89 eV. Theoretically Simulated XRD pattern of LHDN single crystal has been carried out. Vibration frequencies are calculated using B3LYP/6-31+G (d,p) and B3LYP/6-311++ G(d, p) . Vibration mode assignments were also compared with the experimental results. The optimized geometrical parameters, fundamental vibrational frequencies, IR intensity, Raman activity, atomic small charges, dipole moment, reduced mass, force constant and other thermodynamic parameters were calculated. The second harmonic generation (SHG) efficiency has been carried out and it reveals the NLO property of the crystals. The HOMO and LUMO analysis were used to determine the charge transfer within the molecule and quantum chemical parameters related to the LHDN compound.

**Keywords :** Powder XRD, optical absorption, Density Functional Theory, HOMO-LUMO analysis, FTIR, SHG efficiency

## I. INTRODUCTION

Intensive research effort has been concerted on the investigation of the nonlinear optical processes in π-conjugated organic molecules and materials in the recent past decades [1, 2]. The rapid and sustained growth of the field is mainly due to the technological promise of these materials. The utmost importance in the design strategy for efficient non-linear optical (NLO) materials in terms of the molecular design and the supramolecular aggregation is basically aimed to accomplish their potential applications in various photonic technologies. This overwhelming approach crafts a sole field of intriguing explorations in chemical synthesis, molecular and material characterization, theoretical modeling, and NLO studies and photonics technology [3]. The molecular NLO active crystals have been intensively studied to establish the observed structure function correlation through the computational modeling of molecules as the origin of the nonlinear optical response in such systems are governed by the electronic polarizability of the electrons at the molecular level [4] as well as the geometrical arrangement of the NLO-

chromophores present in the molecular system. The sensitive understanding of the structural and electronic response properties of NLO materials have been provided extensively both experimentally and theoretically using the quantum mechanical density functional theory (DFT) approach by vibrational spectroscopy. The molecular structural properties such as their atomistic level energy, vibrational frequencies, transition moment directions, magnitudes of the normal modes of vibrations etc. can be simulated with great accuracies by theoretical computational methods. Considerable effort has been devoted to understand the vibrational, optical, nonlinear response and electronic structure properties of the molecule- based NLO active organic crystals by the DFT based quantum chemical analysis [5]. In this paper, we report the synthesis, crystal structure, spectral and DFT studies of L-Histidine Dinitrate (LHDN) single crystals. Here the structural properties of the title compound were studied experimentally and is compared theoretically. Thus, owing to the industrial and biological significance of substituted quinolines, extensive spectroscopic studies on using Fourier transform infrared (FTIR) and NMR. The DFT calculations with the hybrid exchange-correlation functional B3LYP (Becke's three parameter (B3) exchange in conjunction with the Lee–Yang–Parr's (LYP) correlation functional) which are specifically significant in systems comprising of extensive electron conjugation and/or electron lone pairs [6-9]. Therefore the present investigation has been undertaken to study the vibrational spectra of this molecule entirely and to classify the various modes with greater wave number accuracy. Also, chemical reactivity values such as chemical hardness, chemical potential electro negativity and electrophilicity index. HOMO, LUMO analysis have been used to reveal information regarding charge transfer within the molecule.

## II. MATERIALS AND METHODS

L-Histidine Dinitarte crystals were grown from aqueous solution by slow solvent evaporation technique at room temperature. The starting materials were AR-grade L-histidine and nitric acid. The solution was prepared by dissolving 1 mol of L-histidine and 2 mol of nitric acid in 10 ml of deionised water. The chemical reaction is as follows:

$$C_6H_9N_3O_2 + 2HNO_3 \longrightarrow C_6H_{11}N_3O_2^{+} + 2NO_3^{-}$$

The synthesized compound was dissolved in doubly distilled water using a magnetic stirrer and filtered twice to remove the suspended impurities in the solution. One month later, transparent crystals were obtained. The solubility of the synthesized material of LHDN was carried out at various temperatures (Figure 1). Optically good quality crystals of dimension 31 mm x 3 mm x 10 mm were obtained. The photograph of as grown single crystal of LHDN is shown in Figure 2.

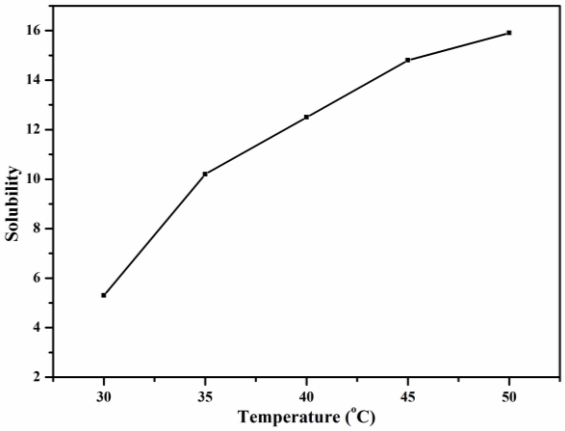


**Figure 1.** Solubility curve of LHDN crystal

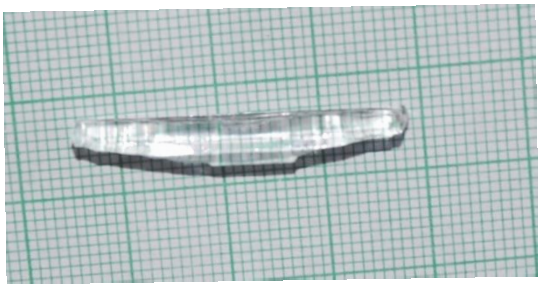

**Figure 2.** Photo graph of as grown LHDN

## III. RESULTS AND DISCUSSION

### 3.1 Powder X-ray diffraction analysis

The crystal structure and purity of L L-Histidine Dinitrate was confirmed by X-ray diffraction measurement. The powder sample of LHDN was subjected to powder X-ray diffraction analysis with a monochromatic Cu Kα radiation (λ = 1.5406 A°). The Bragg's diffraction peaks were indexed for the orthorhombic system. L-Histidine Dinitrate crystallizes in orthorhombic space group $P2_12_12_1$. The cell dimensions are: a = 5.472 (2) Å, b=8.028(3)Å, c=25.138(8)Å, V = 1104.293 (7) $Å^3$. The obtained lattice parameters are in good agreement with the reported values [10]. The observed prominent peaks conform the crystalline property of the grown LHDN crystal. Experimental Powder XRD pattern is shown in Figure 3. Theoretically Simulated XRD pattern of LHDN single crystal is also given in Figure 4.

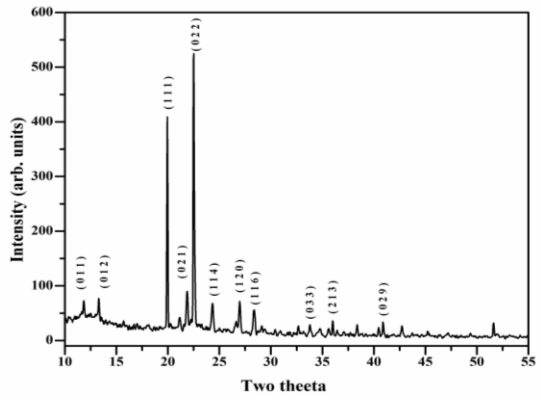


**Figure 3.** Experimentally obtained Powder XRD pattern of LHDN

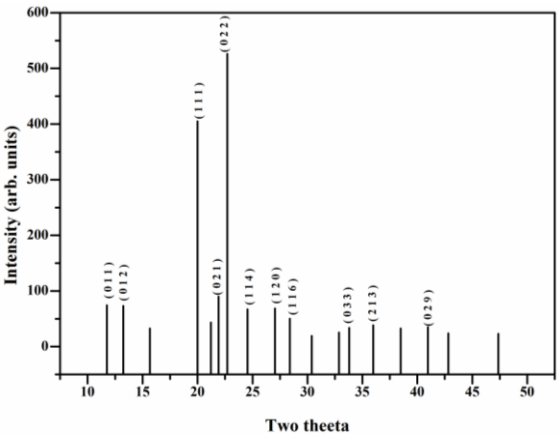


**Figure 4.** Theoretically simulated powder XRD pattern of LHDN

### 3.2 Computational Details

Density functional theory calculations are performed using Gaussian'03 program package [11]. The geometries were fully optimized without any constraint. The vibration frequencies are calculated by using B3LYP/6-31+G(d, p) and B3LYP/6-311++ G(d, p) respectively. Vibration mode assignments were also compared with the experimental results. The optimized geometrical parameters, fundamental vibrational frequencies, IR intensity, the atomic small charges, dipole moment, reduced mass, force constant and other thermodynamic parameters were calculated [12].

#### 3.2.1. Molecular Geometry

The numbering scheme for L - Histidine Dinitrate is shown in Figure 5. The minimum energy was obtained by DFT methods with different basis sets (6-31+G (d, p) and 6-311++G (d, p)) as -1110.1770219a.u, and -1110.495932 a.u., respectively. the comparative optimized structural parameters such as bond lengths and bond angles by DFT-B3LYP with 6-31+G (d, p) and 6-311++G (d, p) basis sets are presented respectively. Calculated geometrical parameters represent good approximation and they are the bases for the calculating other parameters, such as vibrational frequencies and thermodynamics properties.

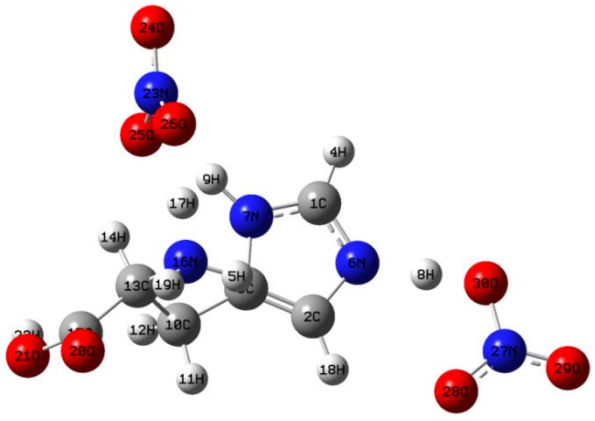


**Figure 5.** Atomic numbering system adapted for ab initio computations of LHDN molecule.

### 3.3. Vibrational assignments

The molecule of LHDN has 30 atoms. It has 84 normal vibrational modes. 56 of these modes should

be symmetric A' and 28 anti symmetric A″, with respect to the reflection on the symmetry plane. For the atoms located in the plane of molecule, the A' vibrational displacements takes place in the plane of the molecule, the A″ modes corresponds to the displacement out of the plane of the molecule.

Γ (3N-6) = 56A' (in – plane) + 28 A″ (out – of plane)

The detailed vibrational assignments of fundamental modes of LHDN FT-IR experimental frequencies are calculated. The experimental FT-IR spectrum was reported in the Figure 6. The theoretically simulated FT-IR spectrum at B3LYP/6-31+G (d, p) and B3LYP/6-311++G (d, p) basis set were shown in Figure 7 and 8.

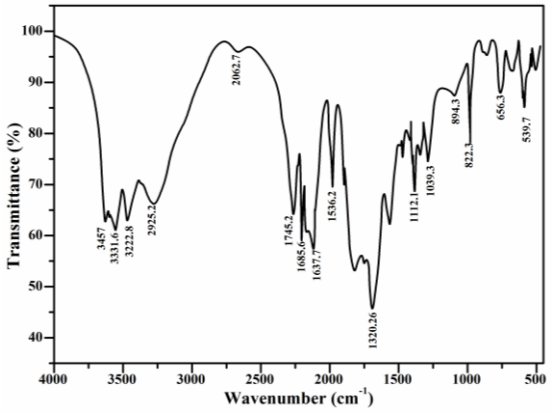


**Figure 6.** Experimental FT-IR Spectrum of LHDN

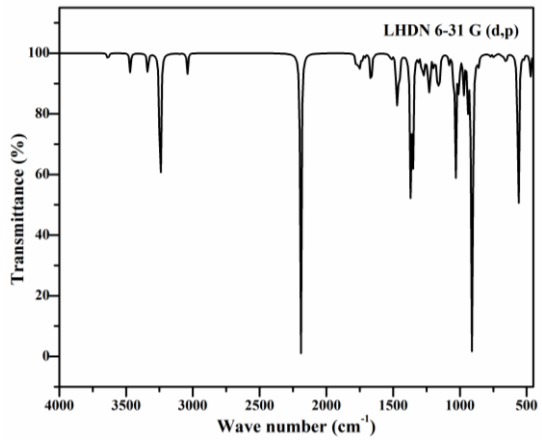


**Figure 7.** Observed FT IR Spectrum of LHDN by 6-31+ G (d, p) method

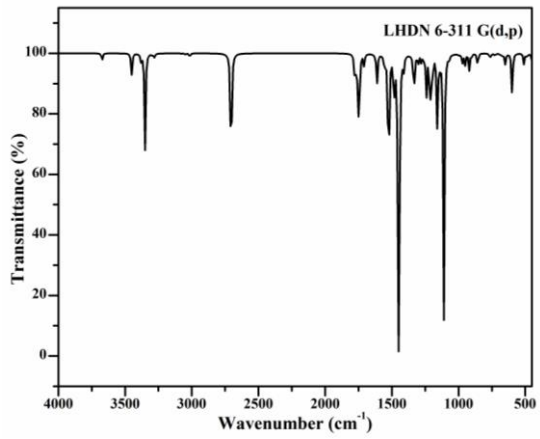


**Figure 8.** Observed FT IR Spectrum of LHDN by 6-311+++ G (d, p) method $NO_3$ Vibrations

### 3.3.1. C=O Vibrations

The stretching vibration C=O is commonly expected in the region 1690 ± 30 $cm^{-1}$. In LHDN, the stretching vibration of C=O band falls at 1685 $cm^{-1}$ for the experimental spectrum and 1665.19 and 1622.6 $cm^{-1}$ for the computed values using 6-31+ G (d, p) and 6-311++ G (d, p) basis sets. The C=O in-plane deformation is expected in the region 645±55 $cm^{-1}$. The bands are observed at 656 in the IR spectrum and at 656.563, 649.332 $cm^{-1}$ theoretically from 6-31+ G (d, p) and 6-311++ G (d, p) basis sets. The C=O out-of-plane deformation is in the range 540±80 $cm^{-1}$ and the DFT calculations give this mode at 522.070 and 508.931 $cm^{-1}$ using the two different basis sets and the experimental value is 539 $cm^{-1}$.

*3.3.2. C=N Vibrations*

The C=N stretching bands are observed in the region 1550-1750$cm^{-1}$. The experimental bands are observed at 1745 for IR and 1754.30, 1752.59 $cm^{-1}$ from the 6-31+ G (d, p), 6-311+++ G (d, p) basis sets [14]. IR spectrum exhibits strong and broad bands due to C=N at 1635$cm^{-1}$. The experimental band was observed at 1637 $cm^{-1}$ and 1644.06, 1610.42 $cm^{-1}$ from the DFT calculations. The C=N stretching skeletal bands are observed in the range 1627-1566 $cm^{-1}$. For LHDN, the band is observed at 1536 $cm^{-1}$ in the spectrum and 1531.27, 1554.60 $cm^{-1}$ using 6-31+ and 6-311++ basis sets. The IR spectrum of the Schiff base showed strong

bands at 1637 $cm^{-1}$ and is assigned to (C=N) stretching vibrations.

The $NO_3$ asymmetric and symmetric stretching vibrations falls at 1389 and 1072 $cm^{-1}$ respectively, and observed frequencies are lowered from the computed values by around 25$cm^{-1}$ which reveals the non-bonded interactions of oxygen atoms of the nitrate groups. For LHDN the same is observed at 1320 $cm^{-1}$ and 1310.49, 1303.05 $cm^{-1}$ from DFT calculation using 6-31+ G (d, p) and 6-311++ G (d, p) basis sets. The nitro group is observed from 1075 $cm^{-1}$and 1080.25, 1110.31 $cm^{-1}$ from the calculated values. Furthermore, these modes are broader and stronger than those of all other modes in the LHDN crystal suggesting that being a strong acceptor these nitrate groups are actively participated in intra and inter molecular ionic hydrogen bonding with the other electron- deficient atoms.

### 3.4. Hyperpolarizability

NLO techniques are considered as one among most the structure-sensitive methods to study molecular structures and assemblies. Since the potential of organic materials for NLO devices have been proven, NLO properties of many of these compounds have been investigated by both experimental and theoretical methods [13]. Quantum chemical calculations have been shown to be useful in the description of the relationship between the electronic structure of the systems and it's NLO response.

The computational approach allows the determination of molecular NLO properties as an inexpensive to design molecules by analyzing their potential before synthesis and to determine the higher order hyperpolarizability tensors of molecules.

The calculated first order hyper polarizability of LHDN is 4.187944 x $10^{-30}$ esu by 6-31+ G (d, p) and 4.07815 x $10^{-30}$ esu by 6-311++ G (d, p) basis sets. The maximum β value may be due to π electron cloud movement from donor to acceptor which makes the molecule highly polarized and the intramolecular charge transfer possible. The dipole moment of the molecule was also calculated with B3LYP/6-31+ G (d, p) & 6-311++ G (d, p) basis sets.

Dipole moment the reflects molecular charge distribution and is given as a vector in three dimensions. Therefore, it can be used as descriptor to depict the charge movement across the molecule depends on centers of the positive and negative charges. Dipole moments are strictly determined for neutral molecules. For charged systems, its value depends on the choice of origin and molecular orientation.

### 3.5. HOMO – LUMO Gap

In principle, there are several ways to calculate the excitation energies. The first, and the simplest one involves the difference between the highest occupied molecular orbital (HOMO) and the lowest unoccupied molecular orbital (LUMO) of a neutral system. This form corresponds to the frozen orbital approximation, the ground state properties are used to calculate the excitation values. The density functional methods (which are based on Hohemberg and Kohn theorem) are designed to yield total energies. HOMO- LUMO orbital picture is shown in Figure 9 and 10.

However, the orbitals in this case (Kohn–Sham orbitals) are not electronic orbitals but mathematical arrangements and eigen values are not directly related to the electronic excitation energies [14]. Nevertheless, it is often a good approximation to neglect these formal inconsistencies and consider them as electronic and orbital energies, as they are in the HF framework [15].

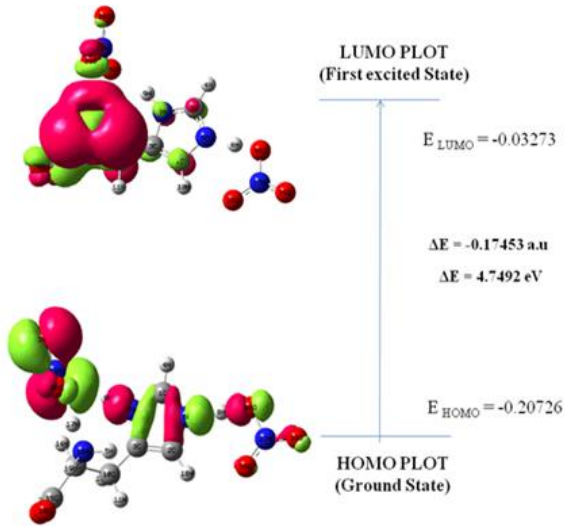


**Figure 9.** HOMO–LUMO plot of LHDN at B3LYP/6-31+G (d, p)

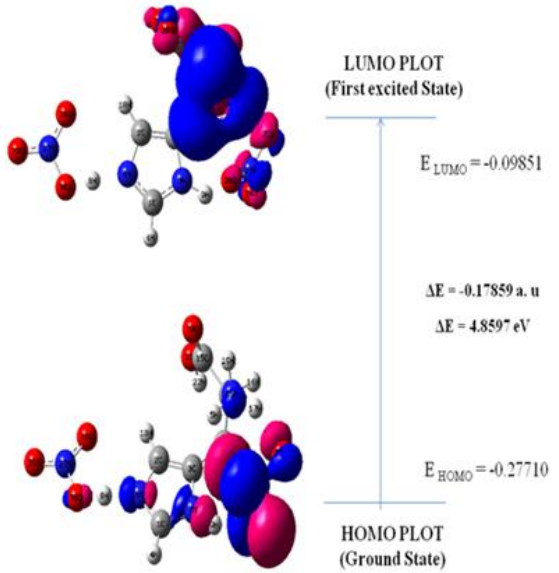


**Figure 10.** HOMO –LUMO plot of LHDN at B3LYP/6-311++G(d,p)

The calculated energy values of HOMO – LUMO are found to be -0.17453 a.u and -0.17859 a.u. The energy gap of HOMO – LUMO explains the eventual charge transfer interaction within the molecule, which influence the first order hyperpolarizabilities.

### 3.6. UV-Vis-NIR spectrum and evaluation of linear optical constants

The recorded transmission spectrum of LHDN shows the lower cutoff wavelength at 240 nm and a wide transparency in the entire visible region which makes the material suitable for second harmonic generation, shown in Figure 11. The variation of $(\alpha h\upsilon)^2$ versus $h\upsilon$ in the fundamental absorption region is plotted in Figure 12 and Eg is evaluated by the extrapolation of the linear part. The band gap is found to be 4.7 eV.

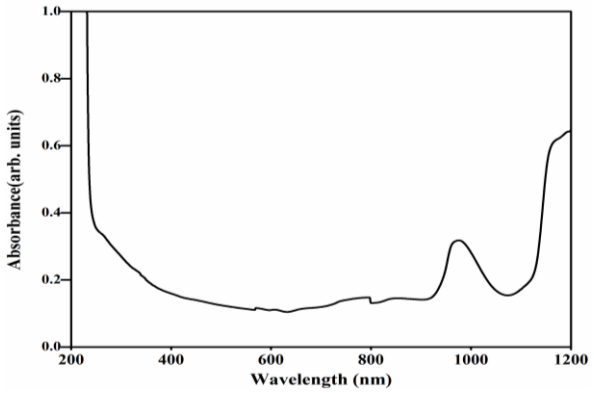


**Figure11.** Optical absorption spectrum of LHDN

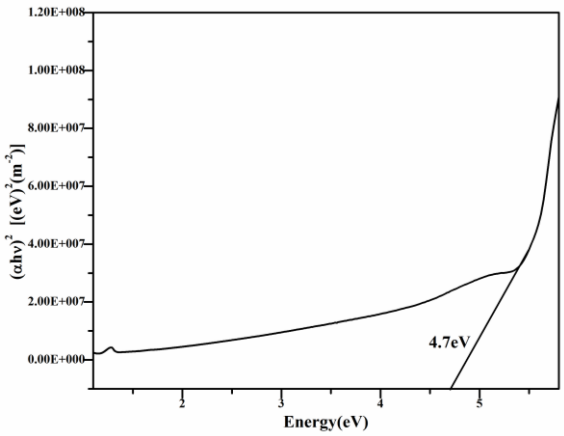


**Figure12.** Energy band gap of LHDN

### 3.7. Vickers Microhardness

Microhardness measurements of LHDN crystal were made using a Vickers diamond pyramidal indenter attached to an incident light microscope. After the preliminary adjustments, the crystal has been mounted properly on the base of the microscope. Now the selected face of (1 0 0) has been indented gently by the loads varying from 10 to 50 g for a dwell period

of 10 s at room temperature. In the present analysis, the indented impressions are approximately pyramidal shape. The shape of the impression depends on its structure, crystal face, etc. The hardness was calculated using the relation

$$Hv = \frac{1.8544P}{d^2} \text{ Kg/mm}^2$$

The load above 50 g develops multiple cracks on the crystal surface due to the release of internal stresses generated locally by indentation. From this experiment, we observed that hardness decreases with increase in load up to 50g. It may be due to the elastic nature of the specimen. The work hardening coefficient has been determined using the relation,

$$P = k_1 d^n$$

and it was found to be 1.517 which shows that the present specimen belongs to harder category. The Figs.13 and 14 give the microhardness profile and work hardening coefficient respectively. Stiffness of the material has been calculated in table 1.

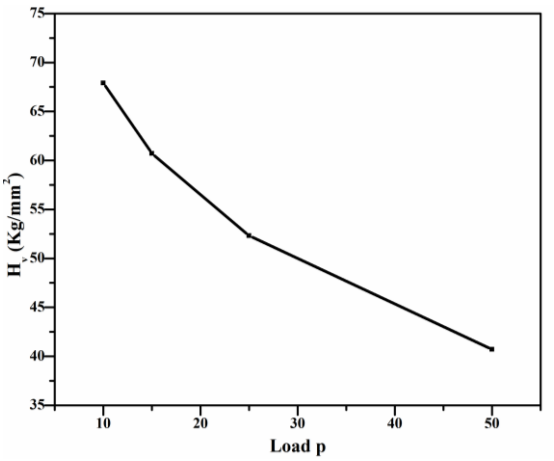


**Figure 13.** Plot of log d Vs log p for LHDN

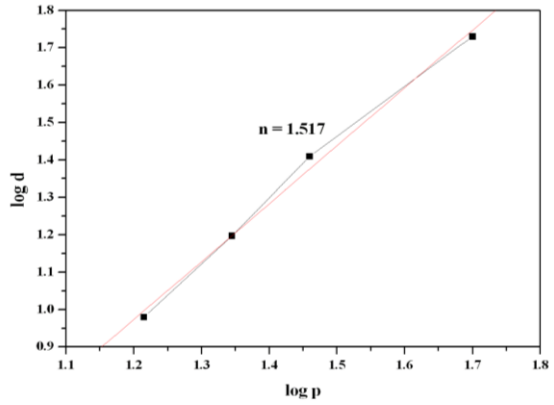


**Figure 14.** Plot of log d Vs log p for LHDN

**Table 1.** Variation of $C_{11}$ with load.

| Load (gm) | Hv (Kg/mm²) | $C_{11}$ (GPa) |
|---|---|---|
| 10 | 67.9 | 1606.098 |
| 15 | 60.7 | 1320.019 |
| 25 | 52.3 | 1017.133 |
| 50 | 40.7 | 655.8284 |

### 3.8. SHG in LHDN crystal

The nonlinear optical conversion efficiency has been carried out using the Kurtz and Perry technique. It is an important and popular tool to evaluate conversion efficiency of a NLO material. A Q-switched Nd: YAG laser operating at the fundamental wavelength 1064 nm, generating about 1.3 mJ and pulse of width 8 ns was used for the present experimental study. The input laser beam was passed on an IR reflector and then directed on the microcrystalline powdered sample of LHDN packed in a capillary tube. The light emitted by the sample was detected by a photodiode detector with oscilloscope assembly. When the laser was passed through LHDN specimen, second harmonic signal of 532 nm is generated it was confirmed by the emission of green light. The second harmonic signal of 991 mW was obtained for LHDN single crystal with reference to KDP (275 mW). Thus, the SHG efficiency of LHDN single crystal is nearly 3.6 times greater than KDP. So the candidate material can be used for frequency conversion in NLO devices.

### 3.9. Dielectric studies

Figure15 and 16 show the variation of dielectric constant and dielectric loss with log frequency. The dielectric constant of the sample was measured for different frequencies. It is observed from the plot that the dielectric constant decreases exponentially with increasing frequency and then attains almost a constant value in the high frequency region starting from 3 KHz to 5 MHz. It is observed that both the

dielectric constant and dielectric loss decrease with increasing frequency. The characteristic of low dielectric constant and dielectric loss with high frequency for a given sample suggests that the sample possesses enhanced optical quality with lesser defects and this parameter is of vital importance for various nonlinear optical materials and their applications.

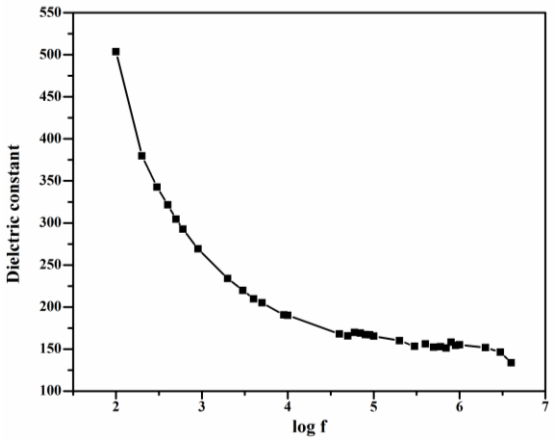


**Figure 15.** Variation of dielectric constant of LHDN

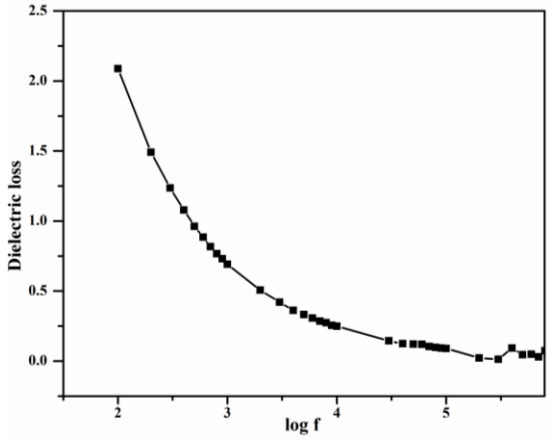


**Figure 16.** Variation of dielectric loss of LHDN

### 3.10. Photoconductivity studies

The variations of dark and photo currents with the applied voltage are measured by increasing the voltage from 0 to 300 V in steps of 20 V for LHDN. Electrical contacts were made on the sample at a known spacing (0.2 cm) using silver paint. Current versus applied field is shown in Figure 17. The plot depicts that both the dark and photo currents increase linearly with the applied field and for a particular applied field, the dark current is found to be higher than the photo current. Thus, LHDN exhibits negative photoconductivity.

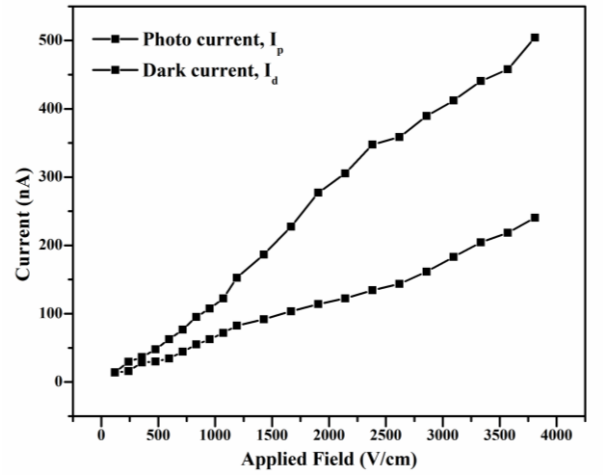


**Figure 17.** Field dependent conductivity of LHDN

## IV. CONCLUSION

Single crystals of LHDN of appreciable size were grown by slow evaporation technique at room temperature. Powder XRD confirmed the grown crystal. Optimized structure of the isolated LHDN molecule obtained by DFT cacultions give the minimum energy state. Existance of strong hydrogen bond in the donor accepter coupling was understood from bond lengths. First order hyperpolarizability of LHDN is calculated as $4.187944 \times 10^{-30}$, $4.07815 \times 10^{-30}$ esu and found useful in molecular designing. Theoretical and experimental Spectroscopic studies exemplify the presence of various functional group in the molecule. Both theoretically simulated and experimentally obtained FT-IR spectra show coincidence. A frontier molecular orbital analysis gives the HOMO-LUMO energy gap value as 4.7492 and 4.8597 eV from different basis sets. The optical absorption spectrum reveals the very low absorption in the entire visible and infrared region of the crystal. The lower UV cut-off wavelength of the sample observed at 240 nm is a desirable parameter for NLO crystals. The NLO property was confirmed using Nd: YAG laser of wavelength 1064 nm and the efficiency was estimated to be 3.6 times higher than that of KDP. The dielectric studies prove the low values of

dielectric constant and dielectric loss in the sample at high frequency. The promising crystal growth characteristics and properties of LHDN crystal indicate it as a potential material for photonic, electro-optic and SHG device application.

## V. REFERENCES


[1]. Sahraoui.B, Rivoire.G, Terkia-Derdra. N, Salle .M, Zaremba J, J. Opt. Soc. Am. B, 1998; 15(2):923-928.

[2]. Ouazzani H. E, Iliopoulos .K, Pranaitis.M, Krupka O, Smokal.V, Kolendo.A, Sahraoui.B, J. Phys. Chem. B 2011; 115: 1944-1949.

[3]. Madhavan. J, Aruna S.K, Prabha. J, Packium Julius , Ginson P Joseph ,Selvakumar .S, Sagayaraj .P, Journal of crystal growth, 2006; 293:409-414.

[4]. Tanak .H, Koysal. Y, Işik. S, Yaman. H, Ahsen .V, Bull. Korean Chem. Soc, 2011; 32(2): 673-680.

[5]. Vaschetto M. E, Retamal B. A, Monkman A. P, J. Mol. Struct. Theochem. 1999; 468: 209-221.

[6]. Timothy Clark, Jayaraman Chandrasekhar, Gunther .W. Spitznagel, Paul Von Ragué Schleyer, J. Comput. Chem. 1983 ; 4: 294.

[7]. Scott Gronert, Chem. Phys. Letter, 1996; 252: 415-418.

[8]. Forsyth. D. A, Sebag .A. B, J. Am. Chem. Soc. 1997; 119: 9483-9494.

[9]. Petrosyan .H. A, Karapetyan .H. A, Yu M. Antipin and Petrosyan A. M, Journal of crystal Growth, 2005; 275: 1919-1925.

[10]. Foresman .J.B, Frish (Ed) E, Exploring chemistry with Electronic structure Methods: a Guide to using Gaussian, (Gaussian Inc., Pittsburg, PA, 1996).

[11]. Mulliken R.S, J. Chem. Phys. 23 (1955) 1833-1840.

[12]. Benali-Cherif, N., Abouimrane, A., Sbai, K., Merazig, H., Cherouana, A. & Bendjeddou, L. (2002). Acta Cryst. E58, o160-o161.

[13]. Hohenberg. P, and Kohn W, Physical Review B, Vol. 136, 1964, pp. 864-871.

[14]. Kohn .W and Sham. L. J, Phys. Rev. 140, A1133 (1965)

[15]. Varsanyi. I. the effect of radurizing radiation doses on low density polyethylene films. Acta Aliment, 1, 1972,297-314.